Scaling up anodic TiO_2 nanotube layers for gas phase photocatalysis

Hanna Sopha[a,b], Michal Baudys[c], Milos Krbal[a], Raul Zazpe[a,b], Jan Prikryl[a], Josef Krysa[c], Jan Macak[a,b,*]

[a]*Center of Materials and Nanotechnologies, Faculty of Chemical Technology, University of Pardubice, Nam. Cs. Legii 565, 53002 Pardubice, Czech Republic*

[b]*Central European Institute of Technology, Brno University of Technology, Purkyňova 123, 612 00 Brno, Czech Republic*

[c]*Department of Inorganic Technology, University of Chemistry and Technology Prague, Technicka 5, 166 28 Prague, Czech Republic*

* Corresponding author: e-mail address: jan.macak@upce.cz (J.M. Macak)

Abstract

In this work, for the first time, an anodic TiO_2 nanotube layer of large area (~50 cm^2), was used for the photocatalysis in the gaseous phase. Hexane was chosen as model pollutant. The nanotube layer showed a superior efficiency compared to a reference TiO_2 layer of the same thickness composed of immobilized P25 nanoparticles. An additional TiO_2 coating of the nanotube layer produced by atomic layer deposition did not show an enhancement of the photocatalytic degradation of hexane due to a decreased active surface area, in contrast to the liquid state photocatalysis under applied external potential.

Keywords: titanium dioxide, nanotubes, large area, photocatalysis, hexane

Introduction

Since the pioneering work of Fujishima and Honda [1] reporting the use of TiO_2 for photocatalytic water splitting, TiO_2 has gained wide interests as an excellent photocatalyst for the decomposition of various organic compounds [2-5]. The mechanism of the photocatalytic activity is based on the formation of electron-hole pairs under UV light illumination, where the electron-hole pairs have an energy sufficiently high to form radicals of high oxidizing power [2-5]. However, a requirement for effective photocatalysis is also a large active surface area of the photocatalyst. Thus, the use of nanostructured TiO_2, such as nanoparticles [6,7], nanorods [8,9], or nanotubes [10-12], prepared by various means, has gained significant attention during the recent years.

In particular, many publications reported the use self-organized TiO_2 nanotube layers for the photocatalytic degradation of pollutants [10,13-16]. These layers can easily be produced by anodization of Ti in an fluoride containing electrolyte [17,18]. The nanotube dimensions can be adjusted by the choice of the anodization parameters, i.e. the electrolyte, anodization potential and anodization time. The main advantage of such TiO_2 nanotube layers is that they strongly adhere to the undelaying Ti substrate. This means that no further immobilization is necessary as in case of nanoparticles. Furthermore, due to the straight alignment of the TiO_2 nanotubes on the Ti substrate an improved charge separation is possible that stems from the uni-directional dimensionality of the nanotubes, resulting in an enhanced performance in photoelectrochemical devices [10,19]. All these prospects are also advantageous for the use in photocatalysis, namely when an external potential is applied.

By now, most publications reported photocatalytic tests just on the laboratory scale, i.e. using relatively small active catalyst areas of a few cm^2. This is due to the difficult control of the anodization process parameters on the big scale. The main problem is the huge current received during the anodization of large substrates. This, in turn, leads to an increase of the electrolyte temperature that may result into dielectric breakdown of the growing nanotube layers. Efficient cooling of the electrolyte during the anodization can prevent this unwanted event. However, just a few reports can be found in the literature showing the anodization of large scale Ti substrates [20-24]. These large scale TiO_2 nanotube layers were so far exclusively employed for the photocatalytical degradation of various pollutants in the aqueous phase.

In this communication, a facile fabrication of large scale (~50 cm^2) TiO_2 nanotube layers and their application in gas phase photocatalysis is shown for the first time. Benefits of the nanotube morphology over the nanoparticulate morphology are clearly demonstrated. Hexane has been chosen as model pollutant because its photocatalytical oxidation is not as fast as that for other gaseous pollutant as butylacetate and toluene [25] and it is a widely occurring atmospheric pollutant [26].

Experimental

Ti foils (Goodfellow, purity 99.6 %, 140 μm thick) were degreased by sonication in isopropanol and acetone and dried in air before use. Afterwards, the Ti foils were anodized in an ethylene glycol based electrolyte containing 176 mM NH_4F (Sigma-Aldrich, reagent grade) and 1.5 vol.% deionized H_2O at 60 V for 4 h with an initial sweeping of 50 mV/s employing a high-voltage potentiostat (PGU-200V, IPS Elektroniklabor GmbH). The

anodized area of the Ti foils was 5 x 10 cm^2. The electrolyte was aged before the anodization [27]. During anodization the electrolyte was cooled to 15 °C using a thermostat. At this temperature the cooling was effective enough to prevent the event of breakdown. At the same time the temperature was high enough not to decrease the nanotube layer thickness strongly [28] or increase the inner wall thickness significantly [29,30]. The electrochemical setup consisted of a two electrode configuration with the Ti foil as working electrode and a Pt foil as counter electrode. After the anodization the nanotube layers were rinsed and sonicated in isopropanol and dried in air. Before their further use the samples were annealed in a muffle oven at 400 °C for 1 h to obtain anatase structure.

On half of the annealed TiO_2 nanotube layers were coated by TiO_2 thin layers by atomic layer deposition (TFS200, Beneq). $TiCl_4$ (electronic grade 99.9998%, STREM) and Millipore deionized water (18 MΩ) were used as the titanium precursor and the oxygen source, respectively. High purity nitrogen (99.9999%) was the carrier and purging gas at a flow rate of 400 standard cubic centimeters minute (sccm). Under these deposition conditions, one growth ALD cycle was defined by the following sequence: $TiCl_4$ pulse (500 ms)-N_2 purge (3 s)-H_2O pulse (500 ms)-N_2 purge (4 s). The TiO_2 nanotube layers were coated by TiO_2 applying 200 cycles which led to a nominal TiO_2 coating thickness of 11 nm (according to the growth rate per ALD cycle, evaluated by ellipsometry) [15]. The deposition processes were carried out at 300 ^oC.

A reference TiO_2 layer of the same thickness was prepared by immobilization of P25 nanoparticles (Evonik Degussa GmbH) on glass supports using drop-casting technique (content of TiO_2 ~ 2.34 mg/cm^2).

The morphologies of all types of TiO_2 layers were characterized by a field-emission scanning electron microscope (FE-SEM JEOL JSM 7500F). The inner diameters, nanotube walls and the thicknesses of the nanotube and nanoparticulate layers were evaluated by statistical analyses of the SEM images using proprietary Nanomeasure software.

The photocurrent measurements were carried out on a part of the large area sample in a three-electrode cell leaving a surface area of 0.28 cm^2 exposed to the light (Ag/AgCl reference electrode, Pt wire as counter electrode, Ti substrate as working electrode) at 0.4 V vs. Ag/AgCl in an aqueous 0.1 M Na_2SO_4 electrolyte and in the spectral range from 300 to 420 nm (5 nm step). The setup consisted of photoelectric spectrophotometer with a 150 W Xe lamp and monochromator (Instytut Fotonowy), and a modular electrochemical system AUTOLAB (PGSTAT 204, Metrohm Autolab B.V., *Nova 1.10* software). The IPCE value for each wavelength was calculated as in our previous work [31,32].

The photocatalytical setup was realised according to the ISO standard (ISO 22197). A scheme of the reactor is shown in Fig. 1. A calibrated gas mixture composed of 100 ppm hexane in N_2 was used as pollutant source (Linde Gas). This mixture was further diluted with humidified air using mass flow controllers (see Fig. 1) to a final mixture of 5 ppm hexane in air that was admitted with flow rate 0.5 dm^3/min to the reactor. The relative humidity (RH) in the reactor was set to 50 %. Analysis of the gaseous mixture was performed by GC-FID (Varian CP-3800 with capillary column CP-Sil 5 CB 15×0.25 (0.25) and flame ionization detector).

The active part of the reactor (photocatalyst area exposed to the reactant) had an area of 5 x 10 cm^2 and the headspace (distance of the glass cover) was 0.5 cm. As a light source, a 25 W black light (UVA) tubular light source (350 nm centre wavelength) was used. The irradiance at the location of the reactor was 1 mW/cm^2 in the wavelength range of 340 to 400 nm.

Results and Discussion

Figure 2 shows SEM images of the TiO_2 nanotube layers with and without ALD TiO_2 coating as well as the reference nanoparticulate P25 layer. The nanotube layers (after annealing, Figure 2a) reveal a homogenous arrangement of the nanotubes on the surface of the Ti foil, with an average inner nanotube diameter of ~63 nm and an average layer thickness of ~4.5 µm. Half of the prepared large area TiO_2 nanotube layers obtained additional TiO_2 coating by ALD (Figure 2b). An ALD TiO_2 coating of 200 cycles (corresponding to ~11 nm thickness) was chosen according to our previous publication [15] as it led to the most effective performance for liquid phase photocatalysis. After the coating with ALD TiO_2 the average inner diameter decreased to ~40 nm. This is in good agreement with the calculated thickness of the ALD TiO_2 layer. At the same time a thickening of the nanotube wall thickness was observed, proving the successful coating of the TiO_2 nanotubes. Moreover, it can be seen that the space in between the nanotubes is clogged after the ALD coating. Since P25 is meanwhile classified as standard material in photocatalysis [33], a P25 nanoparticulate layer was used as reference. As can be seen from the SEM images in Figure 2c and d the nanotube and the nanoparticulate layers were of the same thickness. Figure 2e shows an illustrative photograph of the Ti foil with the TiO_2 nanotube layer on it revealing a size of 5 x 10 cm^2.

Figure 3a and b show the photocurrents and the incident photon-to-current conversion efficiency (IPCE) values measured on the TiO_2 nanotube layers with and without ALD TiO_2

coating and on P25. A clear increase of the photocurrents and IPCE values can be observed for the coated TiO_2 nanotube layer due to the passivation of surface states and improved charge collection efficiency [15]. This confirms the previously published findings that ALD TiO_2 coatings have less defects compared to the uncoated TiO_2 nanotube layers [15]. At the same time, these coatings have a stronger effect on the photocurrents than the decrease of the active surface area in case of the ALD coated TiO_2 nanotube layer. As a result, a more efficient charge carrier separation takes place in the ALD TiO_2 coated TiO_2 nanotube layers and higher photocurrents and IPCE values are received on them in comparison to the uncoated nanotube layers [15]. The P25 layer, on the other hand, shows hardly any photocurrent response. This poor photocurrent behaviour has been reported previously [34,35] and can be explained by the presence of numerous electron traps in the TiO_2 nanoparticles. Furthermore, while the TiO_2 nanotube layers consist of pure anatase (due to the annealing at 400 °C as part of the preparation procedure) [32], the P25 consists of a mixture of anatase and rutile.

Figure 3 c and d show the photocatalytic degradation of hexane according to ISO standard 22197 on the as-prepared (uncoated) and the ALD TiO_2 coated TiO_2 nanotube layers, as well as on the reference P25 nanoparticulate layer. Clearly, in case of the uncoated TiO_2 nanotube layer the highest amount of hexane was decomposed, followed by the nanoparticulate layer. The ALD TiO_2 coated nanotube layer revealed the lowest degradation of hexane. Generally, the higher photocatalytic efficiency of the uncoated TiO_2 nanotube layers compared to the reference P25 nanoparticulate layer can be explained by the larger available contact area of the model pollutant with the TiO_2 photocatalyst and straighter diffusion way of the pollutants within the individual nanotubes, compared to the nanoparticulare P25 layer. The very low photocatalytic efficiency of the ALD coated TiO_2 coated nanotube layer is, however, contradictory to the photocatalytic results obtained in the liquid phase [15]. Nevertheless, the strong decrease in photocatalytic efficiency of the ALD TiO_2 coated nanotube layer compared to both counterparts can be mainly explained by a significant decrease of ~70 % of the active surface area due to the ALD TiO_2 coating, rather than by a change of chemical properties. ~~In addition,~~ The inner diameters of the nanotubes used herein are much smaller than in the previous work [15], i.e. 77 nm vs. 230 nm. This difference is due to the necessity to use different anodization conditions, such as different electrolyte and different anodization potential, to achieve high quality TiO_2 nanotube layer on the large scale in the present case. Thus, additional ALD TiO_2 coatings reduced the active surface area significantly, resulting in

extremely small inner diameters of the nanotubes and clogged intertube space (see SEM images in Figure 2).

For the future work, it is thus necessary to investigate various thicknesses of ALD coatings on those TiO_2 nanotube layers that can be prepared on the large scale.

Conclusions

In summary, for the first time a large area nanotube layer of 50 cm^2 was used for the gas phase photocatalytic decomposition of hexane, according to ISO standard 22197. A superior photocatalytic behaviour and significantly higher photocurrent densities were received for the uncoated TiO_2 nanotube layers compared to a photocatalyst consisting of benchmark P25 nanoparticulate TiO_2 layers of the same thickness. The ALD TiO_2 coated nanotube layers revealed higher photocurrent densities than the uncoated nanotube layers, however, reduced photocatalytic efficiency was found for them due to a significantly reduced active surface area.

Acknowledgements

The authors gratefully acknowledge support from the European Research Council (ERC, project No. 638857) and the Ministry of Education, Youth and Sports of the Czech Republic (projects LM2015082, LQ1601 and LTACH17007).

References

[1] A. Fujishima, K. Honda, Electrochemical photolysis of water at a semiconductor electrode**,** Nature 238 (1972) 37-38.

[2] R. Terzian, N. Serpone, C. Minero, E. Pelizzetti, Photocatalyzed mineralization of cresols in aqueous media with irradiated titania, J. Catalysis 128 (1991) 352-365.

[3] A. L. Linsebigler, G. Lu, J. T. Yates, Photocatalysis on TiO_2 surfaces: principles, mechanisms, and selected results, Chem. Rev. 95 (1995) 735-758.

[4] M.R. Hofmann, S.T. Martin, W. Choi, D.W. Bahnemann, Environmental applications of semiconductor photocatalysis, Chem. Rev. 95 (1995) 69-96.

[5] K. Rajeshwar, Photoelectrochemistry and the environment, J. Appl. Electrochem. 25 (1995) 1067-1082.

[6] C. Kormann, D.W. Bahnemann, M.R. Hoffmann, Preparation and characterization of quantum-size titanium dioxide, J. Phys. Chem. 92 (1988) 5196-5201.

[7] T. A. Kandiel, A. Feldhoff, L. Robben, R. Dillert, D.W. Bahnemann, Tailored titanium dioxide nanomaterials: anatase nanoparticles and brookite nanorods as highly active photocatalysts, Chem. Mater. 22 (2010) 2050-2060.

[8] X. Wang, Z. Li, J. Shi, Y. Yu, One-dimensional titanium dioxide nanomaterials: nanowires, nanorods, and nanobelts, Chem. Rev. 114 (2014) 9346-9384.

[9] X. Peng, A. Chen, Large-scale synthesis and characterization of TiO_2-based nanostructures on Ti substrates, Adv. Funct. Mater. 16 (2006) 1355-1362.

[10] J.M. Macak, M. Zlamal, J. Krysa, P. Schmuki, Self-organized TiO_2 nanotube layers as highly efficient photocatalysts, Small 3 (2007) 300-304.

[11] M. Zlamal, J.M. Macak, P. Schmuki, J. Krysa, Electrochemically assisted photocatalysis on self-organized TiO_2 nanotubes, Electrochem. Commun. 9 (2007) 2822-2826.

[12] T. Kasuga, M. Hiramatsu, A. Hoson, T. Sekino, K. Niihara, Formation of titanium oxide nanotube, Langmuir 14 (1998) 3160-3163.

[13] X. Zhou, N. Liu, P. Schmuki, Photocatalysis with tio2 nanotubes: “Colorful” reactivity and designing site-specific photocatalytic centers into TiO_2 nanotubes. ACS Catalysis 7 (2017) 3210 – 3235.

[14] X. Wang, Y. Li, H. Song, Y. Huang, R. Su, F. Besenbacher, Fluoride concentration controlled TiO_2 nanotubes: the interplay of microstructure and photocatalytic performance. RSC Adv. 6 (2016) 18333-18339.

[15] H. Sopha, M. Krbal, S. Ng, J. Prikryl, R. Zazpe, F.K. Yam, J.M. Macak, Highly efficient photoelectrochemical and photocatalytic anodic TiO_2 nanotubelayers with additional TiO_2 coating, Appl. Mater. Today 9 (2017) 104-110.

[16] S. Ng, M. Krbal, R. Zazpe, J. Prikryl, J. Charvot, F. Dvorak, L. Strizik, S. Slang, H. Sopha, Y. Kosto, V. Matolin, F.K. Yam, F. Bures, J.M. Macak, $MoSe_xO_y$-coated 1D TiO_2 nanotube layers: Efficient interface for light-driven applications, Adv. Mater. Interfaces 5 (2017) 1701146.

[17] J.M. Macak, H. Tsuchiya, A. Ghicov, K. Yasuda, R. Hahn, S. Bauer, P. Schmuki, TiO_2 nanotubes: Self-organized electrochemical formation, properties and applications, Curr. Opin. Solid State Mater. Sci. 11 (2007) 3-18.

[18] K. Lee, A. Mazare, P. Schmuki, One-dimensional titanium dioxide nanomaterials: Nanotubes, Chem. Rev. 114 (2014) 9385-9454.

[19] V. Thavasi, V. Renugopalakrishnan, R. Jose, S. Ramakrishna, Controlled electron injection and transport at materials interfaces in dye sensitized solar cells. Mater. Sci. Eng. R 63 (2009) 81-99.

[20] S. Franz, D. Perego, O. Marchese, M. Bestetti, Photoelectrochemical advanced oxidation processes on nanostructures TiO_2 catalysts: Decolorization of a textile azo-dye, J. Water Chem. Tech. 37 (2015) 108-115.

[21] H.-I. Kim, D. Kim, W. Kim, Y.-C. Ha, S.-J. Sim, S. Kim, W. Choi, Anodic TiO_2 nanotube layer directly formed on the inner surface of Ti pipe for a tubular photocatalytic reactor, Appl. Catalysis A: Gen. 521(2016) 174-181.

[22] J. P. Ghosh, G. Achari, C. H. Langford, Design and evolution of a UV LED photocatalytic reactor using anodized TiO_2 nanotubes, Water Environ. Res. 88 (2016) 785-791.

[23] C. Xiang, L. Sun, Y. Wang, G. Wang, X. Zhao, S. Zhang, Large-scale, uniform, and superhydrophobic titania nanotubes at the inner surface of 1000 mm long titanium tubes, J. Phys. Chem. C 121 (2017) 15448-15455.

[24] E. Mena, M.J. Martin de Vidales, S. Mesones, J. Marugan, Influence of anodization mode on the morphology and photocatalytic activity of TiO_2-NT array large size electrodes, Catalysis Today 313 (2018) 33-39.

[25] F. Moulis, J. Krýsa, Photocatalytic degradation of several VOCs (n-hexane, n-butyl acetate and toluene) on TiO_2 layer in a closed-loop reactor, Catalysis Today 209 (2013) 153-158.

[26] https://toxnet.nlm.nih.gov/

[27] H. Sopha, L. Hromadko, K. Nechvilova, J.M. Macak, Effect of electrolyte age and potential changes on the morphology of TiO_2 nanotubes, J. Electroanal. Chem. 759 (2015) 122-128.

[28] S. Das, H. Sopha, M. Krbal, R. Zazpe, V. Podzemna, J. Prikryl, J. M. Macak, Electrochemical infilling of $CuInSe_2$ within TiO_2 layers and their photoelectrochemical studies, ChemElectroChem 4 (2017) 495-499.

[29] G.D. Sulka, J. Kapusta-Kolodziej, A. Brzozka, M. Jaskula, Anodic growth of TiO_2 nanopore arrays at various temperatures, Electrochimica Acta 104 (2013) 526– 535.

[30] M. Enachi, I. Tiginyanu, V. Sprincean, V. Ursaki, Self-organized nucleation layer for the formation of ordered arrays of double-walled TiO_2 nanotubes with temperature controlled inner diameter, Phys. Stat. Solidi (RRL) 4 (2010) 100-102.

[31] T. Ruff, R. Hahn, P. Schmuki, From Anodic TiO_2 nanotubes to hexagonally ordered TiO_2 nanocolumns, Appl. Surf. Sci. 257 (2011) 8177-8181.

[32] S. Das, R. Zazpe, J. Prikryl, P. Knotek, M. Krbal, H. Sopha, V. Podzemna, J. M. Macak, Influence of annealing temperatures on the properties of low aspect-ratio TiO_2 nanotube layers, Electrochim. Acta 213 (2016) 452-459.

[33] E. Friehsa, Y. AlSalka, R. Jonczyk, A. Lavrentieva, A. Jochums, J.-G. Walter, Frank. Stahl, T. Scheper, D. Bahnemann, Toxicity, phototoxicity and biocidal activity of nanoparticles employed in photocatalysis, J. Photochem. Photobiol. C 29 (2016) 1-28.

[34] G. Waldner, J. Krýsa, J. Jirkovský, G. Grabner, Photoelectrochemical properties of particulate and sol-gel layers, Int. J. Photoenergy 5 (2003) 115-122.

[35] G. Waldner, J. Krýsa, Photocurrents and degradation rates on particulate TiO2 layer. Effect of layer thickness, concentration of oxidizable substance and illumination direction, Electrochimica Acta 50 (2005) 4498–4504.

Figures

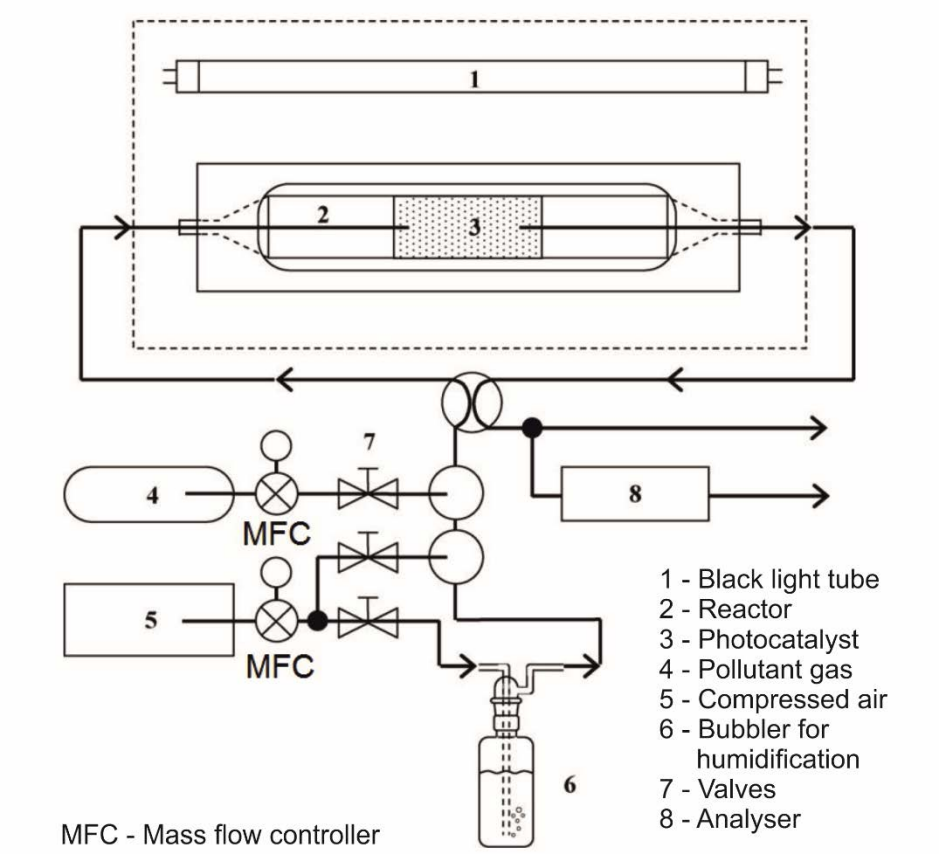

Fig. 1. Apparatus for the evaluation of photocatalytic activity in the gas phase. 1 - black light tube, 2 - reactor, 3 - photocatalyst, 4 - pollutant gas, 5 - compressed (synthetic) air, 6 - bubbler for humidification, 7 - valves, 8 - analyser, MFC - mass flow controller.

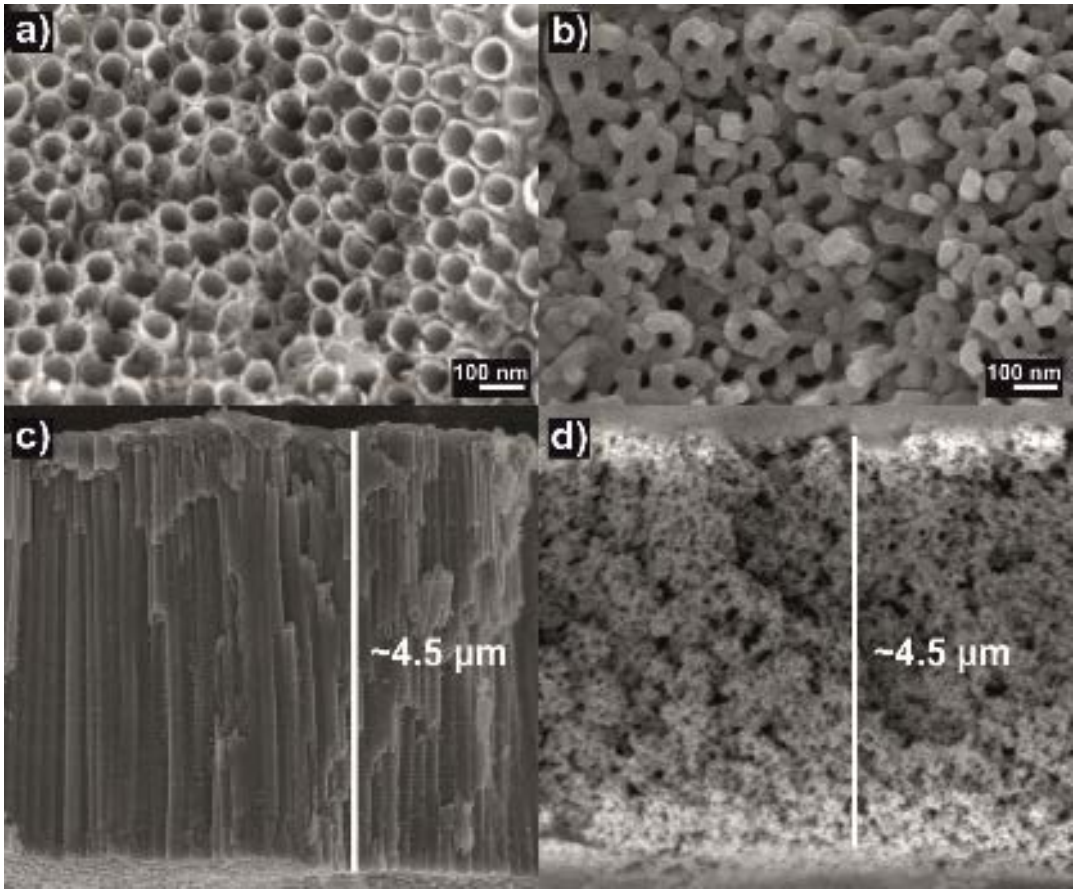

Fig. 2. SEM images of a) the as prepared (uncoated) TiO_2 nanotube layer, b) the ALD TiO_2 coated nanotube layer, c) the cross section of the TiO_2 nanotube layer shown in a, d) the cross section of the nanoparticulate P25 layer, and e) illustrative photograph of the TiO_2 nanotube layer on the Ti foil.

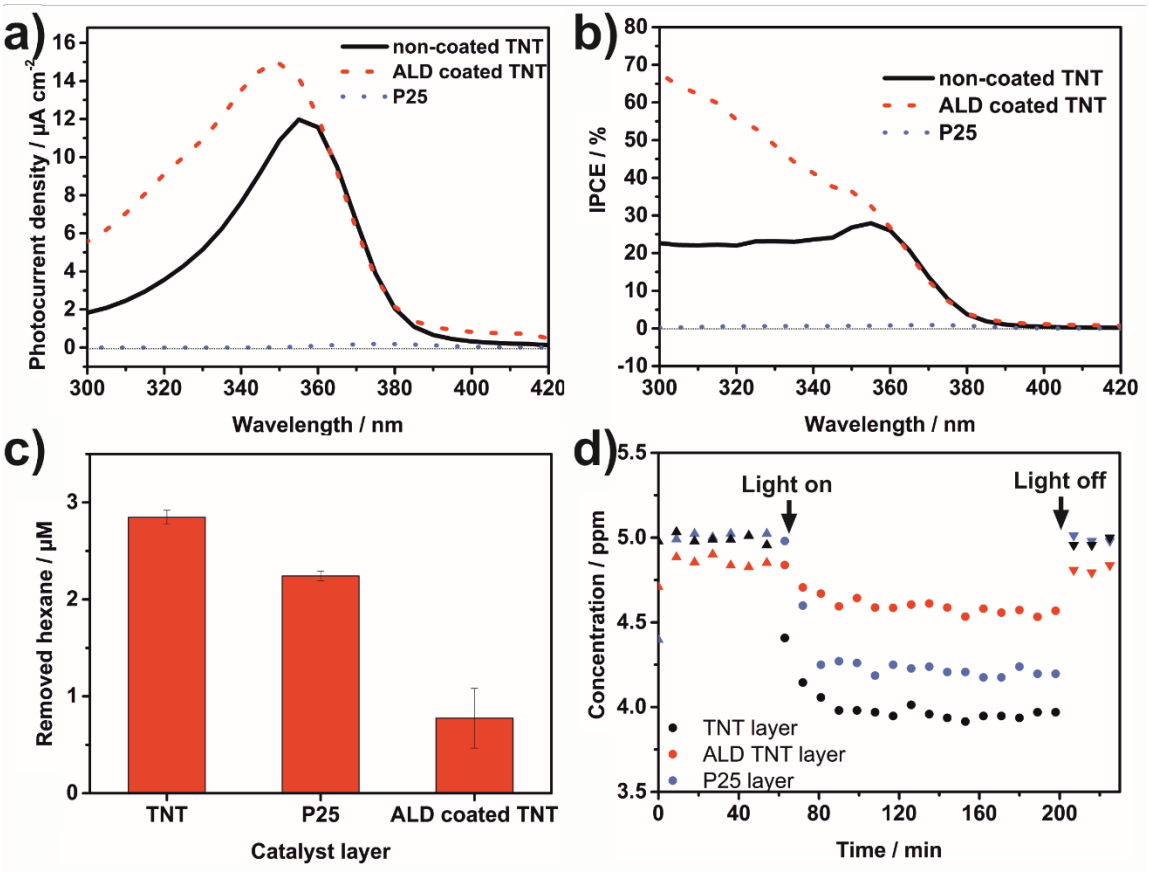

Fig. 3. a) Photocurrent densities (measured at 0.4 V vs. Ag/AgCl) and b) IPCE for the blank and the ALD TiO_2 coated TiO_2 nanotube layers as well as for the P25 layer. A guiding line indicates a photocurrent density of 0 µA cm^{-2} or an IPCE value of 0 %, respectively. c) Hexane removal compared for the three different catalysts and d) concentration changes of hexane in the reactor upon UV light illumination. TNT – TiO_2 nanotube layer.